Optics and Laser Technology 102 (2018) 191–196

Contents lists available at ScienceDirect

Optics and Laser Technology

journal homepage: www.elsevier.com/locate/optlastec

Full length article

Gradient heating protocol for a diode-pumped alkali laser

He Cai [a,b], You Wang [b,*], Juhong Han [b], Hang Yu [b], Kepeng Rong [b], Shunyan Wang [b], Guofei An [b], Hongyuan Wang [b], Wei Zhang [b], Peng Wu [b], Qiang Yu [b]

[a] Beijing Institute of Technology, Beijing 100081, China
[b] Southwest Institute of Technical Physics, Chengdu, Sichuan 610041, China

ARTICLE INFO

Article history:
Received 12 July 2017
Received in revised form 21 September 2017
Accepted 13 December 2017

Keywords:
Gradient heating
Alkali laser
Homogeneous absorption
Window damage

ABSTRACT

A diode-pumped alkali laser (DPAL) has gained rapid development in the recent years. Until now, the structure with single heater has been widely utilized to adjust the temperature of an alkali vapor cell in most of the literatures about DPALs. However, for an end-pumped DPAL using single heater, most pump energy is absorbed by the gain media near the entrance cell window because of the large absorption cross section of atomic alkali. As a result, the temperature in the pumping area around the entrance window will go up rapidly, especially in a case of high pumping density. The temperature rise would bring about some negative influences such as thermal effects and variations in population density. In addition, light scattering and window contamination aroused by the chemical reaction between the alkali vapor and the buffer gas will also affect the output performance of a DPAL system. To find a solution to these problems, we propose a gradient heating approach in which several heaters are tandem-set along the optical axis to anneal an alkali vapor cell. The temperature at the entrance window is adjusted to be lower than that of the other side. By using this novel scheme, one can not only achieve a homogeneous absorption of the pump energy along the cell axis, but also decrease the possibility of the window damage in a DPAL configuration. The theoretical simulation of the laser output features has been carried out for a configuration of multiple heaters. Additionally, the DPAL output performance under different gradient temperatures is also discussed in this paper. The conclusions might be helpful for development of a high-powered and high-beam-quality DPAL.

1. Introduction

A diode-pumped alkali laser (DPAL) has drawn much attention in the past decade [1–5]. As a new kind of hybrid lasers, a DPAL combines the positive features of both a gas laser (GL) and a diode pumped solid state laser (DPSSL). Comparing to conventional high-powered lasers, DPALs offer a number of advantages such as high Stokes efficiency, large optics cross-sections, narrow linewidth and good optical characteristics [6–8]. All these merits make a DPAL one of the most promising candidates of the high-powered laser sources for next generation.

Until now, a lot of experimental studies have been carried out with different kinds of alkali media [9–14]. Krupke et al. demonstrated the first optically pumped alkali vapor laser by using a Ti: sapphire laser as the pump source in 2003 [15]. Then, Page et al. and Wang et al. respectively reported the first LD pumped rubidium vapor laser and cesium vapor laser in 2006 [16,17]. The first diode pumped potassium vapor laser was demonstrated by Zhdanov et al. with two narrow band laser diode arrays [18]. In 2008, Zhdanov et al. performed a Cs DPAL experiment by employing four narrow band LDAs, in which they have achieved an output power of 48 W and an optical–optical efficiency of 49% [19]. Two years later, Zweiback et al. reported an average power of 145 W with a waveguide gain cell configuration [20]. Bogachev et al. have reported the highest output power of approximately 1 kW in a cesium vapor laser in 2012 [21]. In most of these experiments, the structure with single heater has been widely adopted to control the temperature of an alkali vapor cell. However, for an end-pumped DPAL with the single-heater structure, most pump energy is absorbed by the gain media near the entrance window since the absorption cross sections of atomic alkalis are generally very large. Thus, the temperature close to the entrance window will become much higher than those in the other parts. Such a temperature rise will lead to the variation of the vapor density as well as serious thermal effects which are thought to be the main reasons of the power degradation in some DPAL experiments [22]. To solve the problems, we present a novel heating protocol to inhomogeneously anneal the vapor cell in a DPAL system. In this technique, the side wall of the vapor cell is intentionally divided into several

* Corresponding author.
E-mail address: youwang_2007@aliyun.com (Y. Wang).

https://doi.org/10.1016/j.optlastec.2017.12.023
0030-3992/

segments along the cell axis, as diagrammed in Fig. 1. Each segment is heated by a separate heater to realize the gradient heating configuration in a whole. In this way, the saturated alkali number density of a gain medium, which is highly depended on the heating temperature, exhibits the gradient distribution inside a vapor cell. Therefore, a relatively homogeneous absorption of pump energy along the optical axis can be realized by use of this new heating protocol. Additionally, the possibility of the window damage aroused by the chemical reaction between the atomic alkali and the hydrocarbon buffer gas would also decrease as the vapor density near the entrance window is relative low. To our knowledge, there have been no similar reports in the research field of an alkali laser.

In this study, a theoretical model is first set up to analyze the characteristics of an end-pumped DPAL with a gradient temperature configuration. Next, the DPAL features under the different heating conditions are discussed. The theoretical results of the conventional homogenous heating method and the gradient-heating procedure are compared in aspects of the population density at higher excited levels, absorption of pump power, heat generation, and output performance.

2. Theory and method

The electronic energy levels and the main kinetic processes of a rubidium laser are shown in Fig. 2 [23]. The D_2 and D_1 lines are the pump absorption and laser emission lines, Q and γ_{32} stand for the quenching rate and fine-structure mixing rate, respectively. A represents the spontaneous emission rate, where the spontaneous emission rate of the $5^2D_{5/2,\ 3/2}$ and $7^2S_{1/2}$ levels, i.e. the higher excited levels, are assumed to be the same value in the study. n_1, n_2, n_3, n_4 and n_5 are respectively the alkali number densities at the $5^2S_{1/2}$, $5^2P_{1/2}$, $5^2P_{3/2}$, $5^2D_{5/2,\ 3/2}$ & $7^2S_{1/2}$, and the ionized levels.

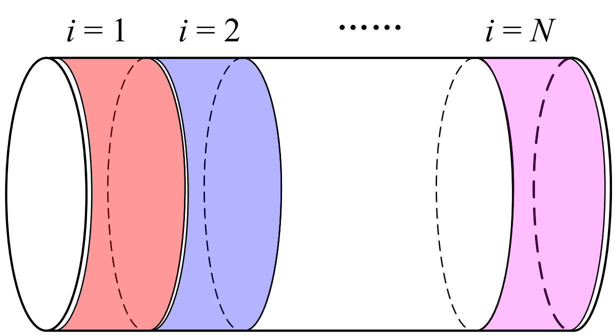

Fig. 1. Schematic illustration of the segmented configuration of a vapor cell.

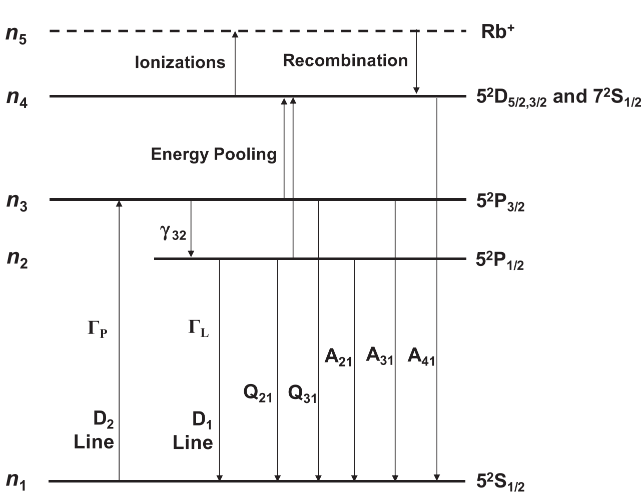

Fig. 2. Energy-level diagram and major kinetic processes of a DPAL.

In the study, we made the following assumptions for mathematical simplicity:

(1) The heat transfer between the adjacent segments of the vapor cell is not taken into account.
(2) Both the temperature and the population density are constants in each segment of the cell.
(3) The temperature variation caused by the generated heat is ignored.

Thus we can obtain the following rate equations that describe the population density distribution in the ith segment of the vapor cell:

$$
\begin{aligned}
\frac{dn_1(i)}{dt} &= -\Gamma_P(i) + \Gamma_L(i) + n_2(i)\times(A_{21}+Q_{21}) + n_3(i)\times(A_{31}+Q_{31}) \\
&\quad + n_4(i)\times A_{41} + k_{EP2}\times(n_2(i))^2 + k_{EP3}\times(n_3(i))^2 + k_{PI}\times n_4(i)\times(n_2(i)+n_3(i)) \\
\frac{dn_2(i)}{dt} &= -\Gamma_L(i) + \gamma_{32}\left[n_3(i) - 2n_2(i)\times\exp\left(-\frac{\Delta E}{k_bT(i)}\right)\right] - n_2(i)\times(A_{21}+Q_{21}) \\
&\quad - 2k_{EP2}\times(n_2(i))^2 - k_{PI}\times n_2(i)\times n_4(i) \\
\frac{dn_3(i)}{dt} &= \Gamma_P(i) - \gamma_{32}\left[n_3(i) - 2n_2(i)\times\exp\left(-\frac{\Delta E}{k_bT(i)}\right)\right] - n_3(i)\times(A_{31}+Q_{31}) \\
&\quad - 2k_{EP3}\times(n_3(i))^2 - k_{PI}\times n_3(i)\times n_4(i) \\
\frac{dn_4(i)}{dt} &= k_{EP2}\times(n_2(i))^2 + k_{EP3}\times(n_3(i))^2 - n_4(i)\times A_{41} - k_{PI}\times n_4(i)\times(n_2(i)+n_3(i)) \\
&\quad - \Gamma_{photoionization}(i) + k_{recombination}\times(n_5(i))^3 \\
\frac{dn_5(i)}{dt} &= k_{PI}\times n_4(i)\times(n_2(i)+n_3(i)) + \Gamma_{photoionization}(i) - k_{recombination}\times(n_5(i))^3 \\
n_0(i) &= n_1(i)+n_2(i)+n_3(i)+n_4(i)+n_5(i) \\
\Gamma_{photoionization}(i) &= n_4(i)\times\sigma_{photoionization}\times\left(\frac{\Gamma_L(i)}{\sigma_{21}(n_2(i)-n_1(i))} + \frac{\Gamma_P(i)}{\sigma_{31}(\lambda)\left(\frac{n_3(i)}{2}-n_1(i)\right)}\right)
\end{aligned}, \tag{1}
$$

where σ_{21} is the collisionally broadened cross section at D_1 line, $\sigma_{31}(\lambda)$ is the spectrally resolved pump-absorption cross section, $\triangle E$ is the energy gap between the $^2P_{3/2}$ and $^2P_{1/2}$ levels, k_b is the Boltzmann constant, $\sigma_{photoionization}$ is the photo-ionization transverse section, $L_g(i)$ is the length of a gain medium in the ith segment, $T(i)$ is the heating temperature which is assumed to be equal to the temperature of the liquid alkali on the wall in the ith segment of the cell, $\Gamma_{photoionization}$ is the photo-ionization transition rate, k_{EP2} and k_{EP3} are the rate constants of the energy pooling of the $5^2P_{1/2}$ and $5^2P_{3/2}$ levels, k_{PI} is the rate coefficient of Penning ionization, and $k_{recombination}$ is the recombination rate constant, respectively.

In Eq. (1), $n_0(i)$ is the total alkali number density in the ith segment and its value is highly depended on the heating temperature. As the density distribution of atomic alkali vapor inside a sealed cell is very complicated for a gradient heating condition, we simply use the following equation to approximately compute the total alkali number density in the ith segment [24]:

$$
n_0(i) = \frac{T(i)}{T_{gas}(i)}\frac{133.322}{k_bT(i)}\times 10^{2.881+4.312-\frac{4040}{T(i)}}, \tag{2}
$$

where $T_{gas}(i)$ is the temperature of the gaseous alkali metal in the cell. In this study, we assumed that the gas temperature $T_{gas}(i)$ is 10 K higher than the liquid alkali temperature $T(i)$ during the simulation.

In Eq. (1), $\Gamma_P(i)$ and $\Gamma_L(i)$ respectively represent the pump absorption rate and laser emission rate in the ith segment of a vapor cell. For an typical end-pumped DPAL as shown in Fig. 3, $\Gamma_P(i)$ and $\Gamma_L(i)$ can be expressed by [25]

$$
\begin{cases}
\Gamma_p(i) = \frac{\eta_{mode}(i)}{V_L(i)}\int\frac{\lambda}{hc}P_p(\lambda,i)\times\left\{1-\exp\left[-\left(n_1(i)-\frac{n_3(i)}{2}\right)\sigma_{31}(\lambda)L_g(i)\right]\right\}d\lambda \\
\Gamma_L(i) = \frac{(P_L^+(i)+P_L^-(i))}{V_L(i)}\frac{\lambda_0}{hc}\times\left\{\exp\left[(n_2(i)-n_1(i))\sigma_{21}L_g(i)\right]-1\right\}
\end{cases}, \tag{3}
$$